Transient Characteristics of a Vertical Grounding Electrode — Experimental Observations and FDTD Simulations

K. Nakamura, A. Ametani, N. Nagaoka and Y. Baba, Doshisha University, Japan

***Abstract*-- This paper investigates transient characteristics of a vertical grounding electrode based on experiments and simulation results by a finite difference time domain (FDTD) method, which is one of the most widely used numerical electromagnetic analysis methods. The simulation results agree with the measured results satisfactorily. The traveling wave velocity from the sending end to the bottom of a vertical electrode is found to depend not only on the earth permittivity but also on the resistivity. In high resistivity earth, the velocity is given by $c_0/\sqrt{(\varepsilon_e)}$ as well-known.**

***Keywords*: grounding, transient, vertical electrode, propagation characteristic, FDTD simulation.**

I. Introduction

A grounding network is essential in a power station and a substation to keep human safety and to guarantee reliable operation of power equipment [1, 2]. The electrode impedance formula is inherent if a circuit theory-based approach such as the EMTP is adopted to analyze the propagation characteristic and the transient response [3, 4]. There exist well-known formulas of the steady-state resistance of horizontal and vertical electrodes derived by Sunde [5, 6]. However, there exists no high frequency impedance formula of the vertical one. Also, the propagation phenomena in a grounding system have not been made clear.

This paper investigates transient characteristics of a vertical grounding electrode based on experiments and simulation results by a finite difference time domain (FDTD) method [7-10], which solves Maxwell's equation directly and can give a solution merely from the geometrical configuration and the physical parameters of a given electrode. The effect of the current lead wire length, the position of a pulse generator and its high resistance representing a current source on the transient characteristic of a vertical electrode is also discussed based on the measurements and FDTD simulation results.

The authors are with the Department of Electrical Engineering, Doshisha University, Kyoto 610-0321, Japan(E-mail;aametani@mail.doshisha.ac.jp;).

Paper submitted to the International Conference on Power Systems Transients (IPST2013) in Vancouver, Canada July 18-20, 2013.

II. Effect of Wire Connecting Electrode and Current Lead Wire

A. Experimental Conditions

Fig.1 illustrates the experimental setup for measuring transient voltages at the top of an electrode. The radius of the electrode is 10 mm and the length is 1 m. For a voltage source, a pulse generator (NoiseKen INS-4040) is used, and an output voltage from a pulse generator (P.G.) is applied to the electrode through a resistance of 5 kΩ, so that the source can be regarded as a current source. An injected current and voltages are measured by using the oscilloscope (Tektronix DPO 4104), the voltage probe (Tek P6139A) and the current probe (Tek CT-2 P6041). Fig.2 shows the injected current waveforms. A current lead wire and a voltage reference wire are kept perpendicular to each other and to the electrode so as to avoid mutual coupling between those as far as possible.

Table I summarizes the experimental and simulation conditions together with measured, simulation and theoretical results. A connecting wire to the electrode in the table is a conductor which connects a current lead wire and a grounding electrode. The detail is explained in Section C (Fig.4). Measured and simulation voltages in Table I correspond to the impedance for the applied current of 1 A and the rise time T_f ≒10 ns, i.e. nearly a step function. The theoretical value of Sunde's formula for a steady-state resistance of a vertical grounding electrode [5, 6] is calculated by the following equation.

$$R_s = (\rho/2\pi x)[ln\{(\sqrt{4x^2+r^2}+2x)/r\} - (\sqrt{4x^2+r^2}-r)/2x] \quad (1)$$

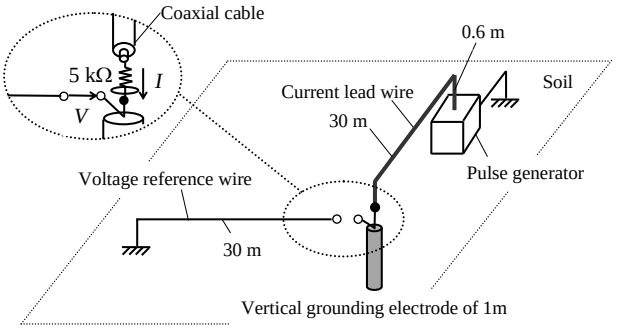

Fig. 1. Experimental setup.

TABLE I
EXPERIMENTAL AND SIMULATION CONDITIONS AND RESULTS

Case	connecting wire to the electrode	measured voltage [V]		simulation voltage [V]		Sunde
		peak / time [ns]	t = 200 ns	peak / time [ns]	t = 200 ns	Rs [Ω]
Case 1	no wire	30.5 / 4.2	12.9	30.2 / 6.1	11.5	12.7
Case 2	covered conductor	63.2 / 5.2	10.1	67.5 / 3.4	10.7	12.7
Case 3	bare conductor	51.3 / 5.2	9.6	46.8 / 6.1	9.7	10.3

Electrode radius r = 0.01 m, ρ_e = 16 Ωm, applied current : rise time T_f = 10 ns, amplitude I_0 = 1 A

In the measurement, I is the injected current, V is the potential difference between the voltage at the top of the electrode and the voltage reference wire.

The earth resistivity of the test yard is 16 Ωm. The Wenner method [4] was utilized to measure the resistivity. The steady-state grounding resistance of the vertical electrode with length 1 m was 13 Ω.

B. Simulation Conditions

Fig.3 shows an analytical space for an FDTD simulation. The dimensions of the analytical space are 5.0 m × 6.0 m × 4.1 m and the cell size is 0.02 m. Liao's 2nd order absorbing boundary is set at the boundaries of the analytical space. The ground level is 2.5 m from the bottom of the analytical space, and the earth resistivity is set to be 16 Ωm with the relative permittivity being 10. The grounding electrodes are assumed to be a perfect conductor. A current lead wire, voltage reference wire and a connecting wire to connect the current lead wire and the electrode are represented by a thin wire model [10]. A covered conductor used as a connecting wire is represented by a conductor covered by an insulator of which the thickness is the same as one cell with the conductivity of 10^{-12} S/m and the relative permittivity of 1. A current waveform in Fig.2 is applied to the top of the electrode as illustrated in Fig.3. The time step Δt of an FDTD simulation is taken to be 0.027 ns, and the maximum observation time is 200 ns.

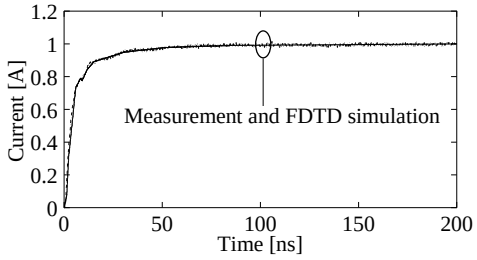

Fig. 2. Injected current.

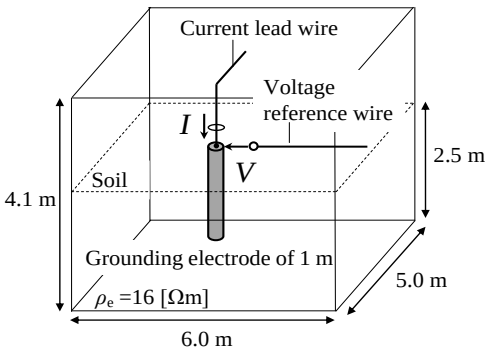

Fig. 3. An analytical space.

C. Measured and Simulation Results

Fig.4 shows measured voltage waveforms for (a) Case 1, (b) Case 2 and (c) Case 3, respectively, together with simulation results. Also, Table I summarizes the transient and steady-state voltages and resistance R_s of the electrode calculated by the Sunde's formula given in eq. (1).

It is observed in Table I that the steady-state voltage in Case 2 and 3 is about 10 V, lower than 12 V in Case 1, the current lead wire connected directly to the electrode. This corresponds to the fact that the deeper the buried depth of the electrode, the smaller the electrode resistance. Those voltages agree well with the Sunde's theoretical values, but eq.(1) requires ample studies of the effect of the buried depth.

It is clear in Fig.4 of experimental and FDTD simulation results that an initial peak voltage at the top of a grounding electrode is produced by the inductance of a grounding wire, which connects the electrode [11].

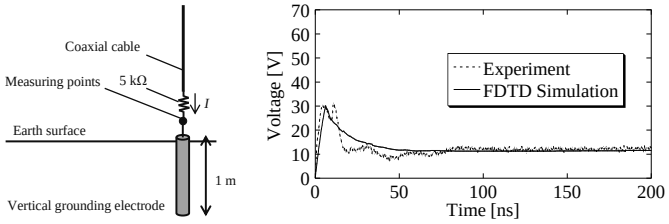

(a) Case 1 : current lead wire connected directly to electrode.

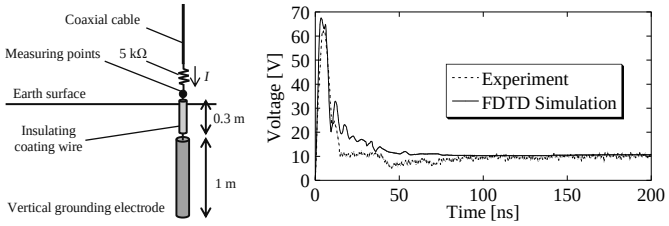

(b) Case 2 : connected by a covered conductor.

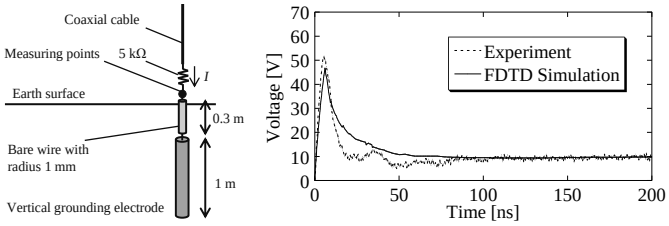

(c) Case 3 : connected by a bare conductor.

Fig. 4. Measured and FDTD simulation results of the voltage at the top of the grounding electrode.

It is obvious in Fig.4 that the FDTD simulation gives satisfactory accuracy in comparison with measured results. Therefore, the FDTD simulation can be used to investigate the transient characteristics of the vertical grounding electrode in the following sections.

III. Effect of a Source Resistance

A. Experimental and Simulation Conditions

In the previous section, the current lead wire and voltage reference wire are assumed as the infinite length wire by connecting conductors with the absorbing boundary. In this section, the experimental setup in Fig.1 is represented by expanding the simulation space in Fig.3 with non-uniform grid of size 0.05 m. The dimensions of the analytical space are 35.5 m × 34.5 m × 6.6 m. The other conditions are the same as those in the previous section. Experiments and simulations are carried out by varying the current lead wire length L from 1 m to 30 m and the locations of the voltage source and source resistance R_0 in Fig.5(1).

B. Measured and Simulation Results

Fig.5 shows the measured and simulation results of the injected current for Cases 1 to 3. Also, Table II summarizes the experimental and simulation conditions, the parameter of the current lead wire length L, the results of the oscillating

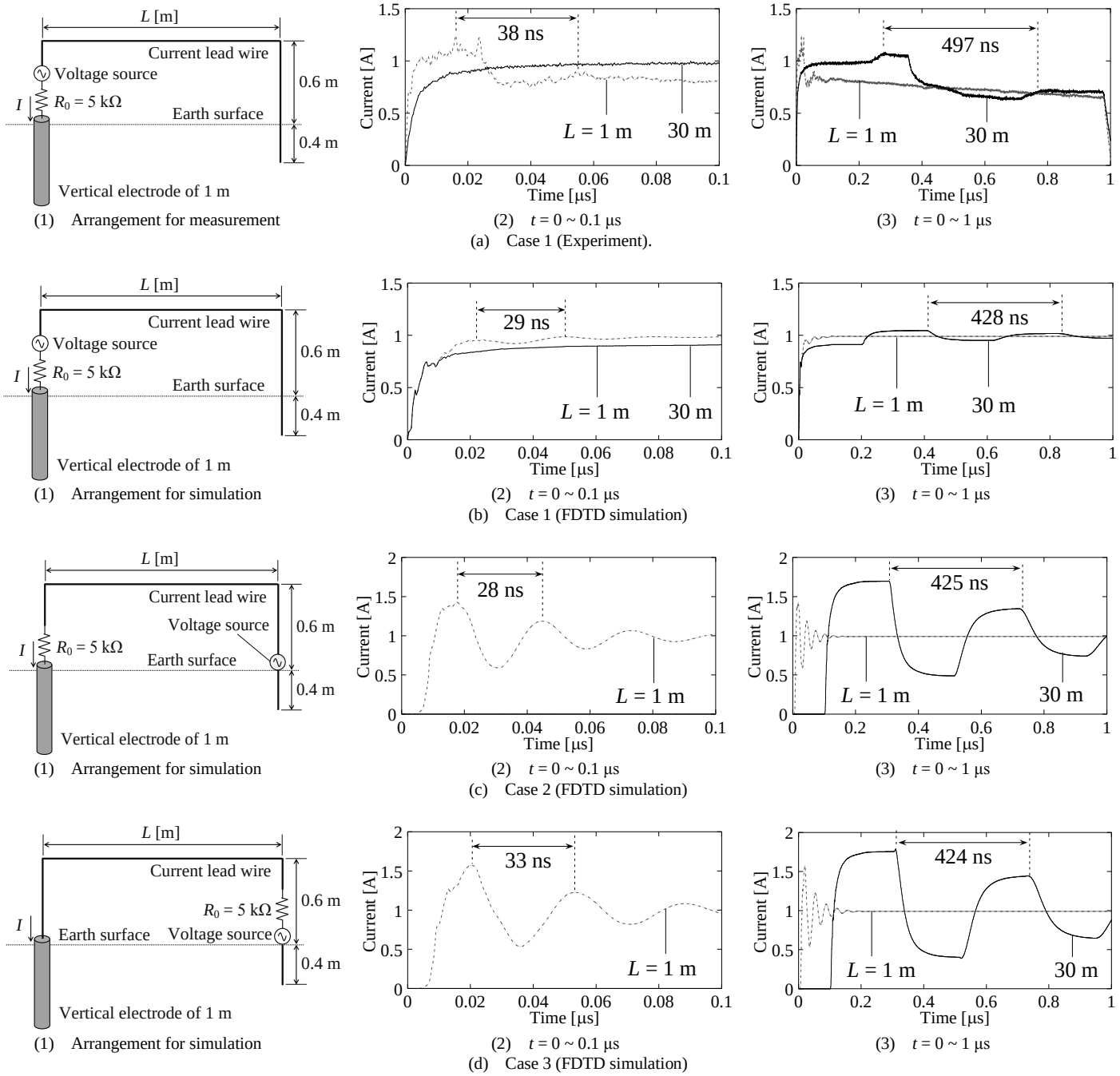

Fig. 5. Experimental and simulation cases and the results of the injected current for Cases 1 to 3.

time period and the traveling time τ, which is determined by the current lead wire length and the velocity of light in free space.

It is observed in Table II that the oscillating time period T is about 4τ. This corresponds to the fact that the oscillations are produced by traveling wave reflection between the source resistance R_0 and the ground of a pulse generator. Thus, it is necessary to take enough length of the current lead wire for the transient response measurement.

It is observed in Fig.5 that the amplitude of the oscillation in Cases 2 and 3 is larger than that in Case 1. This is caused by a reflecting wave from the ground of the pulse generator.

IV. Transient Characteristics in a Vertical Grounding Electrode

A. Simulation Conditions

Fig.6 shows an analytical space for an FDTD simulation. The dimensions of the analytical space are 5.0 m × 5.0 m × 15.0 m with the cell size of 0.05 m. An injected current in Fig.7 is applied to the top of the electrode as illustrated in Fig.6(a) and the current is 1 A with the rise time T_f = 10 ns, i.e. nearly step function. The time step Δt of an FDTD simulation is taken to be 0.067 ns and the maximum observation time is 3 μs. An electrode voltage is calculated by integrating the electric field from the absorbing boundary and the calculation points are $V(d)$ at the inducting electrode as shown in Fig.6(b). Simulations are carried out by varying the earth resistivity from 10 to 1000 Ωm and relative permittivity from 1 to 30.

B. Effects of Earth Parameters

Fig.8 shows simulation results of transient voltages at each depth in the inducing electrode for the varying earth resistivity ρ_e and relative permittivity ε_e.

It is observed in Fig.8 that the voltage waveforms become inductive for the depth less than 2 m, that is, the voltage peak is greater than the steady-state value and appears before the current peak for the depth up to 2 m. When the depth is 10 m, it shows the charging characteristic of a capacitive element. Also, it is clear that the waveforms are not much dependent on the earth permittivity in case of the low earth resistivity. However, such dependency becomes large in case of the high earth resistivity. This is due to the fact that as the earth resistivity becomes high, the grounding electrode is regarded as an isolated conductor. Therefore the traveling waves inside the grounding electrode reach the terminal end and the skin effect becomes apparent. It has been known that the frequency dependence of the earth resistivity and the relative permittivity affect significantly the transient characteristic of a grounding electrode [12-14]. However, it is not clear if the formula of the frequency-dependent parameters proposed in [12] and used in [13,14] is correct. For example, the relative permittivity converges to 1.3 for the frequency reaches zero, and becomes 192 at f = 10 kHz. Thus, the effect of the frequency-dependent parameters is not discussed in this paper. This looks the next step of the present work.

TABLE II
Measured and Simulation Conditions and Results of The Oscillating Time Period

L [m]	τ [ns]	Case 1		Case 2	Case 3
		measured T [ns]	simulation T [ns]	simulation T [ns]	simulation T [ns]
1	7.3	38.2	28.6	27.9	33.0
2	10.7	48.0	41.5	40.4	45.9
5	20.7	97.0	81.5	80.7	86.0
10	37.3	187.8	149.4	149.5	152.8
20	70.7	297.8	286.7	283.0	288.4
30	104.0	497.4	427.9	424.9	423.5

τ : traveling time $\tau = L' / c_0$, $L' = L$ +0.6×2 [m], c_0 = 0.3 [m / ns]
T : oscillating time period

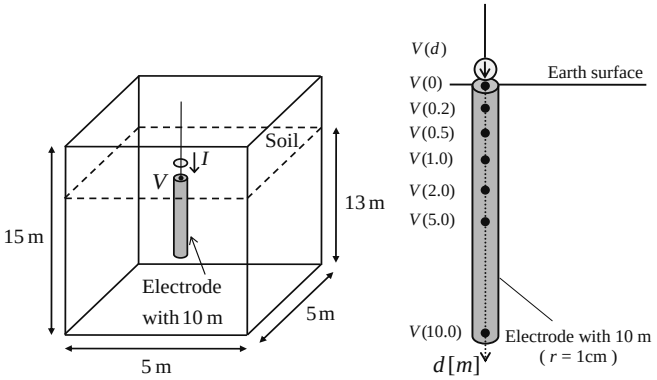

(a) Overall view (b) Side view and calculation points

Fig. 6. An analytical space.

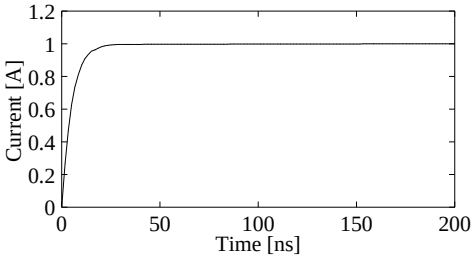

Fig. 7. Injected current.

C. Propagation Characteristics

Fig.9 shows the propagation velocities in the vertical grounding electrode in case of the transient voltages in Fig.8.

It is observed in Fig.9(a) that the propagation velocity becomes independent of the earth permittivity for the depth greater than 2 m. The above observation clearly indicates that the injected current flows into the earth surface in case of the low earth resistivity. Also it is observed in Fig.9 that the propagation velocity in a grounding electrode depends on the velocity of light in vacuum and the earth permittivity as $c_0/\sqrt{(\varepsilon_e)}$ [5, 11] in case of the high earth resistivity.

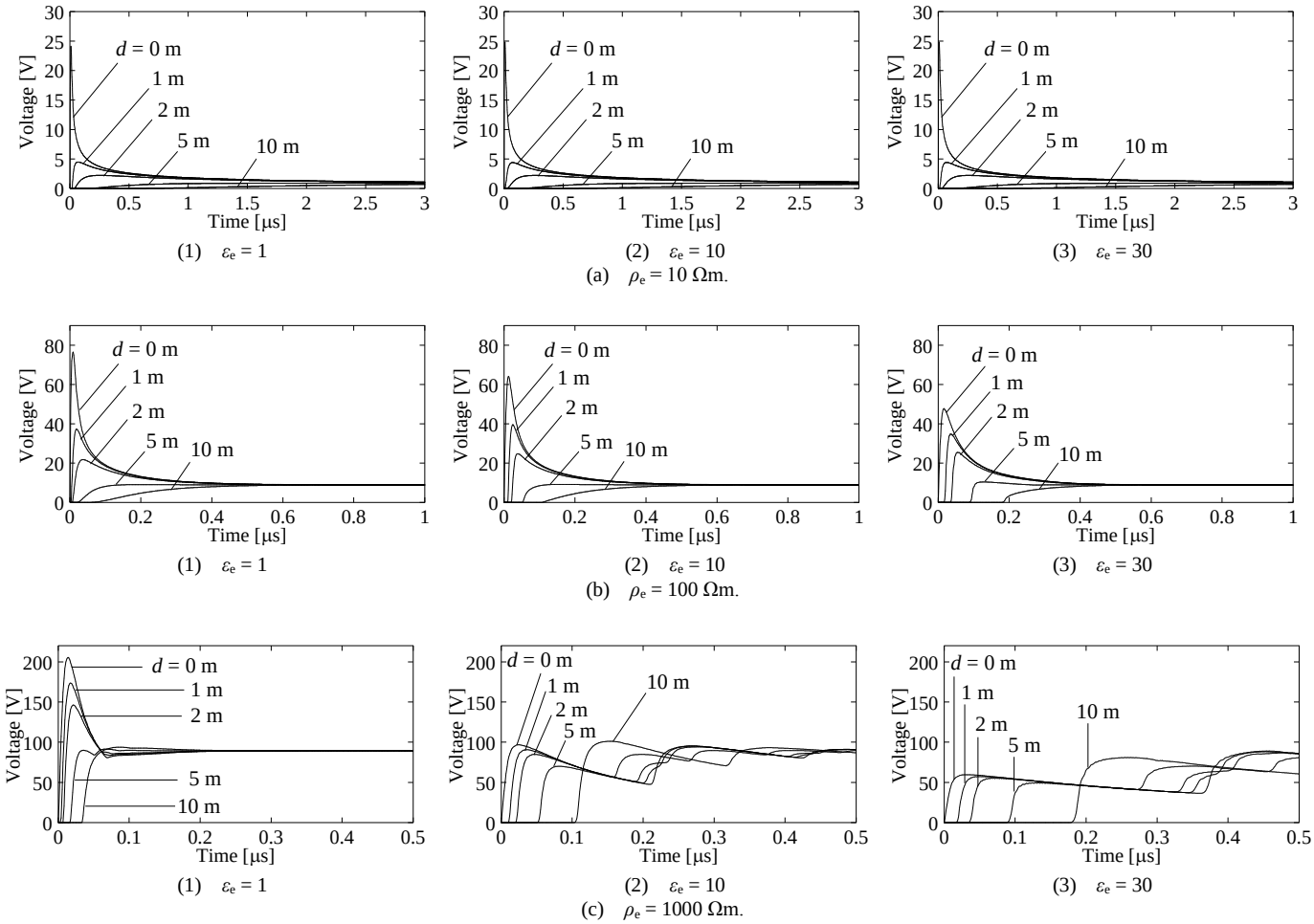

Fig. 8. Simulation results of transient voltages for varying earth resistivity ρ_e and relative permittivity ε_e.

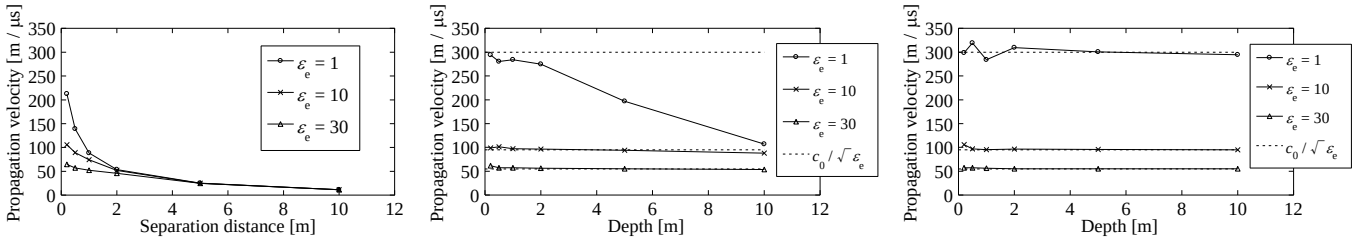

Fig. 9. The propagation velocities in the grounding electrode with ε_e = 1, 10 and 30.

V. CONCLUSIONS

This paper has investigated transient characteristics of a vertical grounding electrode, based on experiments and FDTD simulations. From the investigations, the following remarks are obtained.

(1) An initial peak voltage at the top of a grounding electrode is produced by the inductance of a wire connecting the electrode and a current lead wire.

(2) An oscillation observed in a current waveform is produced by the source resistance and the ground of a pulse generator. Thus, the oscillating period corresponds to a travel time determined by the lead wire length.

(3) The traveling wave velocity from the sending end to the bottom of a vertical electrode is found to depend not only on the earth permittivity but also the resistivity. In a high resistivity earth, the velocity is given by $c_0/\sqrt{(\varepsilon_e)}$ as well-known.

VI. REFERENCES

[1] T. Hosokawa, S. Yokoyama, and T. Yokota, "Study of damages on home electric appliances due to lightning", IEEJ Trans. PE, Vol.125, No.2, pp.221-226 (2005.2) (in Japanese)

[2] T. Hirai, T. Miyazaki, S. Okabe, K. Aiba, and J. Yoshinaga, "A study on an analysis model of grounding electrode for power distribution lines considering transient behavior", IEEJ Trans. PE, Vol.127, No.7, pp.833-839 (2007.7) (in Japanese)

[3] A. Ametani, N. Nagaoka, K. Ueno, T. Funabashi and T. Ueda, "Investigation of Flashover Phases in a Lightning Surge by New Archorn and Tower models" Transmission and Distribution Conference

and Exhibition 2002: Asia Pacific. *IEEE/PES*, vol.2, pp. 1241 – 1246, Oct. 2002

[4] A. Ametani, "Lightning Surge Analysis by EMTP and Numerical Electromagnetic Analysis Method", in *30th International Conference on Lightning Protection - ICLP 2010 Conf*., pp. L1-1 – L1-18.

[5] E. D. Sunde, "Earth conduction effects in transmission system", Dover Publications, Inc., New York (1968)

[6] T. Kawase, Field grounding technology and system, Ohm Pub. Co. (1993) (in Japanese)

[7] T. Uno: Electromagnetic Field and Antenna Analysis by FDTD Method, Corona Pub. Co. (1989) (in Japanese)

[8] Numerical Electro-Magnetic Transient Analysis Method, IEE Japan (2008.3) (in Japanese)

[9] Taku Noda and Shigeru Yokoyama, "Development of a General Surge Analysis Program Based on the FDTD Method", IEEJ Trans. PE, Vol.121, No.5, pp.625-632 (2001) (in Japanese)

[10] Taku Noda and Shigeru Yokoyama, "Thin Wire Representation in Finite Difference Time Domain Surge Simulation", IEEE, Transaction on Power Delivery, Vol.17, pp.840 - 847 (2002)

[11] A. Ametani, H. Morii, and T. Kubo, "Derivation of Theoretical Formulas and an Investigation on Measured Results of Grounding Electrode Transient Responses", IEEJ Trans. PE, Vol.131, No.2, pp.205-214 (2011.2) (in Japanese)

[12] S. Visacro and R. Alipio, "Frequency dependence of soil parameters : Experimental results, predicting formula and influence on the lightning response of grounding electrodes", *IEEE Trans. Power Del*., Vol.27, No.2, pp.927 – 935 (2012.4)

[13] S. Visacro, R. Alipio, M. H. Murta Vale, and C. Pereira, "The response of grounding electrodes to lightning currents : The effect of frequency dependent soil resistivity and permittivity", *IEEE Trans. Electromagn. Compat*., Vol.53, No.2, pp.401 – 406 (2011.5)

[14] M. Akbari, K. Sheshyekani, and M. R. Alemi, "The effect of frequency dependence of soil electrical parameters on the lightning performance of grounding systems", *IEEE Trans. Electromagn. Compat.*, DOI : 10.1109 / TEMC.2012.2222416.